Characterization of poly(*N*,*N*-diethylacrylamide) and cloud points in its aqueous solutions

Ryota Watanabe,[1] Kenichi Takaseki,[1] Motoyuki Katsumata,[1] Daiki Matsushita,[1]

Daichi Ida[2] and Masashi Osa[1]

[1]Department of Chemistry, Aichi University of Education, Kariya, Japan

[2]Department of Polymer Chemistry, Kyoto University, Katsura, Kyoto, Japan

Correspondence: Dr M Osa, Department of Chemistry, Aichi University of Education,

Kariya 448-8542, Japan (E-mail: mosa@auecc.aichi-edu.ac.jp)

ABSTRACT:

The mean-square radius of gyration, second virial coefficient, and intrinsic viscosity were determined in methanol at 25.0 °C for two kinds of poly(*N*,*N*-diethylacrylamide) (PDEA) samples synthesized by radical polymerization in *tert*-butanol and benzene by the use of azobis(isobutyronitrile) as an initiator. Analyses of these quantities showed that the primary structure of both the PDEA samples is linear. The cloud point was also determined in aqueous solutions of the two kinds of PDEA samples. It was found that both for the two kinds of PDEA samples the cloud point decreases with increasing weight-average molecular weight M_w of the sample in contrast to the case of poly(*N*-isopropylacrylamide) (PNIPA) samples previously studied, even though those samples have the same hydrophobic chain-end groups. It was also found that the cloud-point curve of each PDEA sample has a critical point, which has never been found for PNIPA. The critical point was found to move to the upper right with decreasing M_w, as predicted by the conventional polymer solution thermodynamics. It may therefore be concluded that the aqueous PDEA solutions exhibit typical phase behavior of the lower-critical-solution-temperature type which is substantially different from that for aqueous PNIPA solutions.

Keywords: aqueous solution; poly(*N*,*N*-diethylacrylamide); cloud point; phase separation; characterization

Running Heads: Cloud points in aqueous PDEA solutions

INTRODUCTION

It is well-known that aqueous solutions of some water-soluble polymers exhibit lower critical solution temperature (LCST) miscibility behavior that is caused by the breakdown of hydrogen bonds between polymers and surrounding water molecules.[1] Among such water-soluble polymers, poly(*N*-isopropylacrylamide) (PNIPA) has been the most extensively examined from both fundamental and practical points of view, because its aqueous solutions have cloud points near human body temperature,[2] and also because it seems to have potential applications to drug delivery devices and intelligent materials.[3,4]

In recent years, we made a series of rather detailed experimental studies on the phase behavior of aqueous PNIPA solutions,[5-9] and then found that the behavior was not as simple as it is generally considered to be, as follows: (1) The cloud points in aqueous solutions of the PNIPA samples synthesized by radical polymerization with azobis(isobutyronitrile) (AIBN) as an initiator in *tert*-butanol and benzene, which are called PNIPA-T and PNIPA-B samples, respectively, having hydrophobic isobutyronitrile groups at chain ends, are appreciably higher for the PNIPA-T samples than for the PNIPA-B ones, even though the samples have the same weight-average molecular weight M_w and stereochemical composition specified by the fraction f_r of raceme diads.[5] (2) The two kinds of samples have branched structure and the number of branch points is larger for the PNIPA-B samples than for the PNIPA-T ones.[6] (3) The cloud points in aqueous solutions of both the PNIPA-T and PNIPA-B samples decrease with decreasing M_w,[5] which is in contradiction to the prediction on the basis of the conventional polymer solution thermodynamics[10] and is regarded as arising from the effects of their hydrophobic chain-end groups.[7] (4) The cloud points in aqueous solutions of the PNIPA samples synthesized by aqueous redox polymerization, which are called PNIPA-R samples having hydrophilic sulfonate groups at chain ends, are definitely higher than those of the PNIPA-T and

PNIPA-B samples, and increase with decreasing M_w in contrast to the cases of the PNIPA-T and PNIPA-B samples.[9] All these findings indicate that the phase behavior of aqueous PNIPA solutions is governed not only by the hydrogen bonds between PNIPA and surrounding water molecules but also by the end groups and primary structure of PNIPA chains. In addition, Tong *et al.*[11] observed that the cloud points in aqueous solutions for a given PNIPA sample continue to decrease with increasing the PNIPA concentration c in the range of c from 0 up to *ca.*70 wt%, and consequently the minimum point of the cloud point curve (*i.e.* critical point) did not appear. This implicates that the aqueous PNIPA solutions do not necessarily separate into two liquid phases, dilute and concentrated ones, when the temperature is raised above their cloud points.

Under these circumstances, it is desirable to pursue further investigations of aqueous solution behavior of another acrylamide-based polymer, *i.e.*, poly(*N*,*N*-diethylacrylamide) (PDEA), to confirm whether or not the above-mentioned salient features that were found in the phase behavior of aqueous PNIPA solutions are common to them. Thus, we proceed to make a study of aqueous PDEA solutions in the same spirit as that in the previous studies[5-9] for PNIPA. Until now, not a few studies have been performed concerning the phase behavior of aqueous PDEA solutions. Lessard *et al.*[12] have reported molecular weight dependence of cloud point curves of PDEA synthesized by aqueous redox polymerization. Freitag *et al.*,[13] Kobayashi *et al.*,[14,15] and Katsumoto *et al.*[16] have reported effects of stereochemical composition on cloud points of PDEA. Itakura *et al.*[17] have studied aggregation behavior of isotactic PDEA samples in aqueous solutions by using light scattering techniques. Maeda *et al.*[18] investigated changes in hydration states of PDEA during phase transition by using infrared spectroscopy. However, effects of chain-end groups and primary structure of PDEA chains on phase behavior of aqueous PDEA solutions have not yet been studied. Moreover, none of the prior researchers has shown clearly existence of critical point in phase diagram of aqueous PDEA solutions. Therefore, in

this study, we first prepare PDEA samples by radical polymerization with AIBN in *tert*-butanol and benzene, as in the cases of the PNIPA samples. Subsequently, we characterize the PDEA samples so prepared to confirm their primary structure by analyzing the mean-square radius of gyration $\langle S^2 \rangle$ and second virial coefficient A_2, determined from light scattering (LS) measurements, and the intrinsic viscosity $[\eta]$, determined from viscosity measurements, all in methanol at 25.0 °C. We also determine the values of f_r of the PDEA samples from ^{13}C NMR spectra. We then determine the cloud points in the aqueous solutions of the two kinds of PDEA samples, to examine the effects of the hydrophobic chain-ends and the primary structure of the PDEA samples on phase behavior of their aqueous solutions, and also to confirm whether or not their cloud point curves have critical points.

EXPERIMENTAL PROCEDURE

Materials

We synthesized two kinds of original PDEA samples by radical polymerization in *tert*-butanol and benzene by the use of AIBN as an initiator. In each solvent, *N*,*N*-diethylacrylamide (Kohjin Co., Ltd, Tokyo, Japan), which had been purified by distillation under reduced pressure, was polymerized with AIBN under argon at 60 °C for 24 h. The original samples so synthesized were purified by reprecipitaion from acetone solutions into hexane. The resulting polymers were then dissolved in pure water and dialyzed seven times against pure water for 24 h using a cellulose tube. We separated the original samples so prepared into fractions of narrow molecular weight distribution by fractional precipitation using acetone as a solvent and hexane as a precipitant. We dissolved each of the test samples so prepared in 1,4-dioxane, then filtered it through a Teflon membrane of pore size 0.45 μm, and finally

freeze-dried it from their 1,4-dioxane solutions. We note that almost all the chain ends of the PDEA samples are considered to be the hydrophobic isobutyronitrile groups derived from AIBN.

The codes of all the 21 samples used in this work are given in the first column of Table 1, where the PDEA samples synthesized in *tert*-butanol and benzene are generally called PDEA-T and PDEA-B samples, respectively. The values of the ratio of M_w to the number-average molecular weight M_n are given in the second column of the table, which were determined using analytical gel permeation chromatography (GPC) with two serially connected columns, SB-805HQ and SB-804HQ (Showa Denko KK, Tokyo, Japan), connected to a L-7100 solvent delivery pump (Hitachi, Ltd, Tokyo, Japan) and a RI-930 refractive index detector (JASCO Corporation, Tokyo). We used *N*,*N*-dimethylformamide (DMF) containing 10mM lithium bromide at 50 °C as an eluent, and 12 standard polystyrene samples (Tosoh Corporation, Tokyo, Japan, M_w=550–5.46 × 10^6) as reference standards.

We purified the solvent methanol used for LS and viscosity measurements by distillation. The solvent DMF used for analytical GPC was of reagent grade without further purification. The solvent deuterated chloroform used for ^{13}C NMR spectroscopy was of reagent grade without further purification. Water used for the determinations of the cloud points was highly purified through an Autopure WT101UV water purification system (Yamato Scientific Co., Ltd, Tokyo, Japan), and its resistivity was 18.2 MΩ·cm.

Light scattering

We carried out LS measurements to determine M_w and A_2 for all the 21 PDEA samples and $\langle S^2 \rangle$ for 15 PDEA samples with $M_w \gtrsim 2.5 \times 10^5$, in methanol at 25.0 °C. We conducted the

measurements using a Wyatt DAWN EOS multi-angle laser light-scattering (MALLS) detector (Wyatt Technology Corporation, Santa Barbara, CA) with incident light of wavelength 690 nm in micro-batch mode. The MALLS detector was calibrated with pure toluene and normalized with *ca*. 1 wt% methanol solution of a poly(ethylene glycol) sample with $M_w \simeq 8 \times 10^3$ (MP Biomedicals, LLC., Solon, OH). The scattered intensity was measured at five different concentrations for each sample. The obtained data were processed by using the Berry square-root plot.[19] (Some typical examples of the Berry square-root plots for the PDEA samples in methanol at 25.0 °C are shown in the Supporting Information.)

We prepared the most concentrated solution of each sample gravimetrically and made it homogeneous by continuous stirring at room temperature for 1 or 2 days. We purified it optically by filtration through a Teflon membrane with a pore size 0.1 μm. We obtained the solutions of lower concentration by successive dilution. The polymer mass concentrations c of the test solutions were calculated from the weight concentrations of the solutions using the density of the solvent methanol. We used the literature value 0.7866 g/cm^3 for the density of methanol at 25.0 °C.[20]

We measured the refractive index increment $\partial n/\partial c$ at a wavelength of 690 nm using an interferometric refractometer OPTILAB DSP (Wyatt Technology Corporation). The refractometer was calibrated with aqueous solutions of anhydrous sodium chloride. The values of $\partial n/\partial c$ in methanol at 25.0 °C were determined to be 0.175 cm^3/g for all the PDEA samples.

Viscosity

We carried out viscosity measurements for 5 PDEA-T samples (PDEA-T16, PDEA-T27, PDEA-T40, PDEA-T80, and PDEA-T139) and 5 PDEA-B samples (PDEA-B18, PDEA-B28,

PDEA-B51, PDEA-B115, and PDEA-B158) in methanol at 25.0 °C by the use of a conventionally capillary viscometer of the Ubbelohde type. We measured the flow time to a precision of 0.1 s, keeping the difference between those of the solvent and solution larger than 20 s. The test solutions were maintained at a constant temperature within ±0.01 °C during the measurements.

We prepared the most concentrated solution of each sample in the same manner as in the case of the LS measurements. We obtained the solutions of lower concentrations by successive dilution. We calculated the polymer mass concentrations c from the weight fractions with the density of the solvent methanol. The data obtained for the specific viscosity η_{sp} and the relative viscosity η_r were processed as usual by the Huggins (η_{sp}/c vs c) and Fuoss–Mead ($\ln\eta_r/c$ vs c) plots, respectively, to determine $[\eta]$ and the Huggins coefficient k'. (Some typical examples of the Huggins and Fuoss–Mead plots for the PDEA samples in methanol at 25.0 °C are shown in the Supporting Information.)

^{13}C NMR

We recorded ^{13}C NMR spectra for 2 PDEA-T samples (PDEA-T7 and PDEA-T139) and 2 PDEA-B samples (PDEA-B28 and PDEA-B122) in deuterated chloroform at 50 °C at *ca.* 2 wt% on a spectrometer JEOL JNM ECA-600 (JEOL Ltd, Tokyo, Japan) at 150.9 MHz using an rf pulse angle of 90° and a pulse repetition time of 10 s. A total of 22000 spectra was accumulated for each sample. We added tetramethylsilane to each solution as an internal standard.

Transmittance of light

We measured the intensity of light passing through aqueous solutions of 6 PDEA-T

samples (PDEA-T7, PDEA-T11, PDEA-T27, PDEA-T40, PDEA-T80, and PDEA-T139) and 4 PDEA-B samples (PDEA-B18, PDEA-B28, PDEA-B85, and PDEA-B122) at various weight fractions *w* ranging from 0.5 to 25 wt% using a home-made apparatus, which was constructed previously,[5,21] with an incident light of wavelength 650 nm that was emitted from a laser diode module. A given test solution contained in a cylindrical cell of diameter 10 mm was immersed in a water bath and stirred continuously. To determine the cloud point of each solution, we increased the temperature of the solution at a rate of *ca*. 1.5 °C/h. During continuous temperature elevation from *ca.* 26 °C to *ca.* 34 °C, the intensity of light passing through the test solution was monitored by a photodiode. The output of the photodiode, along with the solution temperature measured simultaneously was recorded on a personal computer. Then we determined the relative transmittance, defined as the ratio of the intensity of light through the test solution at a given temperature to the intensity at a lower temperature (for which the test solution is transparent), as a function of temperature.

We prepared the most concentrated solution of each sample gravimetrically and made it homogeneous by continuous stirring for 2 days at room temperature. We obtained the solutions of lower concentration by successive dilution.

RESULTS AND DISCUSSION

Characterization

Stereochemical Compositions.

Figure 1 shows ^{13}C NMR spectra for the 4 samples PDEA-T7, PDEA-T139, PDEA-B28, and PDEA-B122 in the range of the chemical shift δ from 173.3 to 174.5 ppm, where signals from the carbonyl carbon in the side group are observed. According to Kobayashi *et al*.,[15] the

signals at 173.4–173.7 ppm, 173.7–174.0 ppm, and 174.0–174.3 ppm are assigned to the isotactic (*mm*), heterotactic (*mr*), and syndiotactic (*rr*) triads, respectively, although they are overlapped partly to each other. To separate the signals into the contributions from the three kinds of triads (*mm*, *mr*, and *rr*), we assume that the spectra at δ=173.3–174.5 ppm are represented by a linear combination of three Lorentzians and then determine the coefficient (or weight) and also the half-width at half-maximum of each Lorentzian by numerical deconvolution, under the constraint that the maximum points of the first, second, and third Lorentzians are located in the ranges of 173.4 ppm ≤ δ ≤ 173.7 ppm, 173.7 ppm ≤ δ ≤ 174.0 ppm, and 174.0 ppm ≤ δ ≤ 174.3 ppm, respectively. From the values of the weight of the three Lorentzians so determined, we estimated the fractions of the triads, which we denote by f_{mm}, f_{mr}, and f_{rr}, for the 4 samples, as follows; $f_{mm} = 0.02_5$, $f_{mr} = 0.74_1$, and $f_{rr} = 0.23_4$ for the sample PDEA-T7, $f_{mm} = 0.00_8$, $f_{mr} = 0.74_6$, and $f_{rr} = 0.24_6$ for the sample PDEA-T139, $f_{mm} = 0.01_5$, $f_{mr} = 0.93_7$, and $f_{rr} = 0.04_8$ for the sample PDEA-B28, and $f_{mm} = 0.03_4$, $f_{mr} = 0.89_4$, and $f_{rr} = 0.07_2$ for the sample PDEA-B122. In Figure 1, the dashed, dot-dashed, and dotted curves represent the Lorentzian components for the *mm*, *mr*, and *rr* triads, respectively. [The ^{13}C NMR spectra including the superimposed values (*mm* + *mr* + *rr*) as well as the Lorentzian components for the three kinds of triads for these four PDEA samples are shown in the Supporting Information.] In the third column of Table 1 are given the values of f_r calculated from the equation,

$$f_r = f_{rr} + \frac{f_{mr}}{2}$$

with the values of f_{mr} and f_{rr} given above. It is seen that the PDEA-T samples have the value *ca*. 0.61 of f_r and the PDEA-B samples have the value *ca*. 0.52 of f_r, indicating that the former samples are more syndiotactic than the latter ones.

Mean-square radius of gyration and second virial coefficient in methanol at 25.0 °C.

The values of M_w and A_2 determined from LS measurements in methanol at 25.0 °C for all the 21 samples are given in the fourth and fifth columns of Table 1, respectively. The sixth column of Table 1 gives the values of $\langle S^2 \rangle$ for the 7 PDEA-T samples, PDEA-T27 through PDEA-T139, and the 8 PDEA-B samples, PDEA-B28 through PDEA-B158, determined simultaneously from the LS measurements in methanol at 25.0 °C. We note that the values of $\langle S^2 \rangle$ for the samples with $M_w \lesssim 2.5 \times 10^5$ have been excluded because the slopes of the Berry square-root plots against the square of the magnitude of the scattering vector for those samples are not sufficiently large to evaluate $\langle S^2 \rangle$ accurately. The values of A_2 are of order 10^{-4} cm^3mol/g^2, indicating that methanol at 25.0°C is a good solvent for PDEA.

Figure 2 shows double-logarithmic plots of $\langle S^2 \rangle$ (in nm^2) against M_w for PDEA in methanol at 25.0 °C. The unfilled circles and triangles represent the values for the PDEA-T and PDEA-B samples, respectively. It is seen from the figure that the values of $\langle S^2 \rangle$ for the two kinds of PDEA samples are in rather good agreement with each other. This agreement implies that the difference in the stereochemical compositions between the two kinds of PDEA samples, as shown in the last subsection, does not appreciably affect the average chain dimension of PDEA in methanol at 25.0 °C. It is also seen that the all the data points follow a straight line of slope 1.2, which is represented by the solid line in the figure, over the whole range of M_w examined. The value 1.2 of the slope is consistent with that for linear[22,23] and also star[24] flexible polymers with very large M_w in good solvents. Thus, these results indicate that the two kinds of PDEA behave as flexible polymers in methanol at 25.0 °C, and there is no difference in the degree of branching between the two kinds of PDEA samples, in contrast to the previous case[6] of PNIPA. We note that, in the case of PNIPA previously studied,[6] the PNIPA samples synthesized by radical polymerization have branched structures and the number of branch points is larger for

the PNIPA-B samples (synthesized in benzene) than for the PNIPA-T samples (synthesized in *tert*-butanol), and consequently the former PNIPA samples have smaller values of $\langle S^2 \rangle$ than the latter PNIPA ones when compared at the same M_w (see Figure 1 in Kawaguchi *et al.*[6]).

Figure 3 shows double-logarithmic plots of A_2 (in $cm^3\ mol/g^2$) against M_w for PDEA in methanol at 25.0 °C. The symbols have the same meaning as those in Figure 2. The values of A_2 for the two kinds of PDEA samples are in rather good agreement with each other, as in the case of $\langle S^2 \rangle$. The quantity of A_2 is proportional to an effective volume excluded to a polymer chain by the presence of another, and therefore the agreement of A_2 between the two kinds of PDEA samples indicates that the effective volume of a given PDEA-T sample is almost the same as that of a given PDEA-B sample with the same M_w. In addition, the data points are seen to follow a straight line of slope −0.2, which is represented by the solid line in the figure, except for the range of small M_w ($\lesssim 10^5$) where the effects of chain ends on A_2 becomes appreciable.[23] The value −0.2 of the slope is consistent with that for linear[22,23] and also star[24] flexible polymers with very large M_w in good solvents, as in the case of $\langle S^2 \rangle$. Further, the values of the interpenetration function Ψ defined as $\Psi = A_2 M_w^2 / 4\pi^{3/2} N_A \langle S^2 \rangle^{3/2}$ with N_A the Avogadro constant estimated for the two kinds of PDEA samples using the values of M_w, $\langle S^2 \rangle$, and A_2 given in Table 1 are consistent with those for the linear flexible polymers[22,23] and definitely smaller than those for the star flexible polymers.[24] Thus, all these results indicate that both the two kinds of PDEA are linear flexible polymers.

Intrinsic viscosity in methanol at 25.0 ℃.

The values of $[\eta]$ and k' determined from viscosity measurements in methanol at 25.0 °C are given in the seventh and eighth columns, respectively, of Table 1. Figure 4 shows

double-logarithmic plots of $[\eta]$ (in dL/g) against M_w for PDEA in methanol at 25.0 °C. The symbols have the same meaning as those in Figures 2 and 3. As in the cases of $\langle S^2 \rangle$ and A_2 shown in Figures 2 and 3, the data points for the two kinds of PDEA samples agree well with each other and follow a straight line of slope 0.7, which is represented by the solid line in the figure, over the whole range of M_w examined. The value 0.7 of the slope is consistent with that for linear[25] and star[24] flexible polymers with very large M_w in good solvents. Further, the values of the Flory–Fox factor Φ defined as $\Phi = M_w[\eta]/(6\langle S^2 \rangle)^{3/2}$ estimated for the two kinds of PDEA samples using the values of M_w, $\langle S^2 \rangle$, and $[\eta]$ given in Table 1 are consistent with those for the linear flexible polymers in good solvents.[22] Therefore, it may be reconfirmed that the two kinds of PDEA are linear flexible polymers. We note that, in the previous case for PNIPA,[6] the values of $[\eta]$ for the PNIPA-B samples are definitely smaller than those for the PNIPA-T samples at the same M_w, since the degree of branching is larger for the former PNIPA samples than for the latter PNIPA ones (see Figure 3 in Kawaguchi *et al*.[6]).

Cloud point in aqueous solutions

Figure 5 shows plots of the (relative) transmittance against temperature for the aqueous solutions of the 6 PDEA-T samples, PDEA-T7, PDEA-T11, PDEA-T27, PDEA-T40, PDEA-T80, and PDEA-T139, at the weight fraction w = 2.72, 3.01, 2.89, 3.02, 3.03, and 3.03 %, respectively. We note that the shape of the transmittance curve for each solution is almost independent of the rate of increase in temperature if it is slower than 1.5 °C/h. It is seen that the transmittance curve shifts toward the left (low-temperature side) with increasing M_w in contrast to the case of the aqueous solutions of the PNIPA-T samples previously studied,[5] in spite of the fact that both the samples were synthesized in the same solvent, *tert*-butanol, and have the same

hydrophobic (isobutyronitrile) chain-end groups. Figure 6 shows plots of the (relative) transmittance against temperature for the aqueous solutions of the 4 PDEA-B samples, PDEA-B18, PDEA-B28, PDEA-B85, and PDEA-B122, at w = 3.14, 3.00, 3.02, and 2.99 %, respectively. As in the case of the PDEA-T samples, the transmittance curve for the PDEA-B samples is seen to shift toward the left (low-temperature side) with increasing M_w. Also in this case, the M_w dependence is in contrast to the case of the aqueous solutions of the PNIPA-B samples previously studied,[5] although both the samples were synthesized in benzene and have the same hydrophobic isobutyronitrile groups at their chain ends.

The cloud point in a given test solution is, in principle, determined to be the temperature at which the solution just starts to become turbid. However, it is somewhat difficult to determine such a temperature unambiguously because the transmittance for each solution starts to decrease from 100% rather gently, as seen from Figures 5 and 6. Therefore, following the previous studies for PNIPA,[5,9] the cloud point in each solution is determined as the temperature at which the transmittance becomes the threshold value 90%, for convenience. The cloud points for the aqueous solutions of the 6 PDEA-T samples (PDEA-T7, PDEA-T11, PDEA-T27, PDEA-T40, PDEA-T80, and PDEA-T139) and the 4 PDEA-B samples (PDEA-B18, PDEA-B28, PDEA-B85, and PDEA-B122) at other w's are also determined in the same manner as mentioned above.

Figure 7 shows the cloud-point curves in aqueous solutions of the PDEA-T samples, PDEA-T7 (○), PDEA-T11 (△), PDEA-T27 (▽), PDEA-T40 (□), PDEA-T80 (◊), and PDEA-T139 (⊕). The solid curves connect smoothly the cloud points for the respective PDEA-T samples. As expected from the result shown in Figure 5, the cloud point at a given w decreases as M_w is increased, which is consistent with the familiar conclusion derived from the polymer solution thermodynamics[10] and in contrast to the previous result[5] obtained for the

PNIPA-T samples. We note that the increase of the cloud point with increasing M_w observed for the PNIPA-T samples may be regarded as arising from the effects of their hydrophobic (isobutyronitrile) chain-end groups.[5,7] On the other hand, in the present case of the PDEA-T samples, the same hydrophobic chain-end groups are considered to have little influence on the behavior of the cloud point of the PDEA-T samples. The reason for the difference in the chain-end effects on the cloud point between PNIPA and PDEA is not clear at present. An investigation of this problem is one of the future works. It is more important to note that the cloud point curve for each PDEA-T sample has a critical point, which has never been observed for aqueous PNIPA solutions.[11] Namely, the cloud point for each PDEA-T sample is seen to decrease with increasing *w* up to the critical point and then increase inversely at the critical point. The existence of the critical points on the cloud point curves means that the aqueous solutions of the PDEA-T samples exhibit liquid-liquid phase separation into two liquid phases, *i.e.*, dilute and concentrated ones, as the temperature is raised above the cloud points. As a matter of fact, the phase separation was observed for all the aqueous solutions of the PDEA-T samples examined. As an example, Figure 8 shows a photograph of the aqueous solution of the sample PDEA-T11 at *ca*. 10% and at *ca*. 34 °C, which exhibits the phase separation into two transparent liquid phases. It is also seen from Figure 7 that the critical point associated with each cloud-point curve tends to move to the upper right as M_w is decreased. Such behavior is easy to understand on the basis of the conventional polymer solution thermodynamics.[10] Therefore, it may be concluded that the aqueous solution of the PDEA-T samples has the typical (and normal) phase diagram of LCST type which is substantially different from that for the PNIPA-T samples.

Figure 9 shows the cloud-point curves in aqueous solutions of the PDEA-B samples, PDEA-B18 (●), PDEA-B28 (▲), PDEA-B85 (▼), and PDEA-B122 (■). The solid curves

connect smoothly the cloud points for the respective PDEA-B samples. As in the above case of the PDEA-T samples, it is seen that the cloud point for the PDEA-B samples at a given w decreases with increasing M_w and that the cloud-point curve for each PDEA-B sample has a critical point. The critical point is seen to move to the upper right as M_w is decreased. From these observations, it may be concluded that the aqueous solutions of the PDEA-B samples also exhibit the typical (and normal) phase behavior of LCST type as well as those of the PDEA-T samples.

In the previous case of PNIPA, it has been found that the cloud point in aqueous solution of the PNIPA-B sample is lower than that of the PNIPA-T one at the same M_w, even though the two kinds of PNIPA samples have the same hydrophobic chain end groups and almost the same value of f_r.[5] The difference in the cloud point between the PNIPA-T and PNIPA-B samples have been considered to be caused by the difference in the degree of branching between them, the number of branch points being smaller for the former than for the latter.[6] Increase in the number of branch points necessarily occurs with increase in the number of the hydrophobic chain-end groups, which may be the reason for the difference in the cloud point between the PNIPA-T and PNIPA-B samples. Under such circumstances, it is therefore interesting to compare the cloud points for the two kinds of PDEA samples used in the present study. Figure 10 shows plots of the critical point temperature against $M_w^{-1/2}$ for the aqueous solutions of the 6 PDEA-T samples (PDEA-T7, PDEA-T11, PDEA-T27, PDEA-T40, PDEA-T80, and PDEA-T139) and the 4 PDEA-B samples (PDEA-B18, PDEA-B28, PDEA-B85, and PDEA-B122). The unfilled circles and triangles represent the values for the PDEA-T and PDEA-B samples, respectively. Strictly speaking the critical point temperature for each sample should be defined as the minimum of its cloud-point curve, but, in this study, it was determined as the lowest value of the cloud points measured for each sample, for convenience. The solid curve connects smoothly the data points

for each kind of PDEA. In the whole range of M_w examined, the critical point temperature is higher for the PDEA-B samples than for the PDEA-T ones when compared at the same M_w, indicating that the cloud point for the PDEA-B samples is generally higher than that for the PDEA-T samples. In the previous subsection, we confirmed that the primary structure of both the PDEA-T and PDEA-B samples is linear and the two kinds of PDEA samples have no branch points, whereas the stereochemical composition for the two kinds of samples is different from each other, the PDEA-T samples being more syndiotactic than the PDEA-B samples. According to Kobayashi *et al.*[15] and Katsumoto *et al.*,[16] the cloud point in aqueous PDEA solutions decreases as syndiotacticity (or f_r) of the PDEA samples used is increased. Therefore, it may be concluded that the difference in the cloud point between the PDEA-T and PDEA-B samples, both having the linear primary structure and the same hydrophobic chain-end groups, is caused by the difference in the stereochemical composition between the two kinds of PDEA samples.

CONCLUSION

We have determined $\langle S^2 \rangle$, A_2, and $[\eta]$ in methanol at 25.0 °C for the two kinds of PDEA samples synthesized by radical polymerization in *tert*-butanol and benzene by the use of AIBN as an initiator, which we call PDEA-T and PDEA-B samples, respectively. It has been found for all of $\langle S^2 \rangle$, A_2, and $[\eta]$ that their values for the two kinds of PDEA samples agree well with each other in the whole range of M_w examined. It has also been found that the slopes of the double-logarithmic plots of these quantities against M_w and also the values of Ψ and Φ are consistent with those for linear flexible polymers with large M_w in good solvents. From these results, it is reasonably considered that the primary structure of both the PDEA-T and PDEA-B samples is linear. We have also determined the values of f_r for the two kinds of PDEA samples

by ^{13}C NMR spectroscopy. Then, it has been found that the PDEA-T samples are more syndiotactic than the PDEA-B samples.

For the aqueous solutions of the PDEA-T and PDEA-B samples, the cloud-point curves have been determined in the range of the weight fraction w from 0.5 % up to 25 %. It has been found that the cloud point at a given w decreases with increasing M_w for either of the two kinds of PDEA samples, this M_w dependence being in contrast to the previous cases[5] of the PNIPA samples synthesized in *tert*-butanol and benzene with AIBN as an initiator. It has also been found that the cloud-point curve for each PDEA sample has a critical point and the aqueous solutions of the PDEA samples exhibit the phase separation into two transparent liquid phases, which has never been observed in the case of aqueous PNIPA solutions. The critical point for either of the PDEA-T and PDEA-B samples is found to move to the upper right with decreasing M_w, as predicted from the conventional polymer solution thermodynamics.[10] Therefore, it may be concluded that the aqueous solution of either of the PDEA-T and PDEA-B samples has the typical (and normal) phase diagram of the LCST type which is substantially different from that for aqueous PNIPA solutions. Furthermore, it has also been found that the cloud point is generally higher for the PDEA-B samples than for the PDEA-T samples, even though both the samples have the same hydrophobic chain-end groups and no branch point. The difference in the cloud point between the two kinds of PDEA samples is regarded as arising from the difference in the stereochemical composition between them.

REFERENCES

1. Koningsveld, R., Stockmayer, W. H. & Nies, E. *Polymer Phase Diagrams* (Oxford University Press, New York, 2001).

2. Schild, H. G. Poly(*N*-isopropylacrylamide): experiment, theory, and application. *Prog. Polym. Sci.* **17**, 163–249 (1992).

3. Kikuchi, A. & Okano, T. Pulsatile drug release control using hydrogels. *Adv. Drug Delivery Rev.* **54**, 53–77 (2002).

4. Gil, E. S. & Hudson, S. M. Stimuli-responsive polymers and their bioconjugates. *Prog. Polym. Sci.* **29**, 1173–1222 (2004).

5. Kawaguchi, T., Kojima, Y., Osa, M. & Yoshizaki, T. Cloud points in aqueous poly(*N*-isopropylacrylamide) solutions. *Polym. J.* **40**, 455–459 (2008).

6. Kawaguchi, T., Kojima, Y., Osa, M. & Yoshizaki, T. Primary structure of poly(*N*-isopropylacrylamide) synthesized by radical polymerization. Effects of polymerization solvents. *Polym. J.* **40**, 528–533 (2008).

7. Kobayashi, K., Yamada, S., Nagaoka, K., Kawaguchi, T., Osa, M. & Yoshizaki, T. Characterization of linear poly(*N*-isopropylacrylamide) and cloud points in its aqueous solutions. *Polym. J.* **41**, 416–424 (2009).

8. Kawaguchi, T., Kobayashi, K., Osa, M. & Yoshizaki, T. Is a "cloud-point curve" in aqueous poly(*N*-isopropylacrylamide) solution binodal? *J. Phys. Chem. B* **113**, 5440–5447 (2009).

9. Ise, T., Nagaoka, K., Osa, M. & Yoshizaki, T. Cloud points in aqueous solutions of poly(*N*-isopropylacrylamide) synthesized by aqueous redox polymerization. *Polym. J.* **43**, 164–170 (2011).

10. Flory, P. J. *Principles of Polymer Chemistry* (Cornell University Press, Ithaca, NY, 1953).

11. Tong, Z., Zeng, F. & Zheng, X. Inverse molecular weight dependence of cloud points for aqueous poly(*N*-isopropylacrylamide) solutions. *Macromolecules* **32**, 4488–4490 (1999).

12. Lessard, D. G., Ousalem, M. & Zhu, X. X. Effect of the molecular weight on the lower critical solution temperature of poly(*N,N*-diethylacrylamide) in aqueous solutions. *Can. J. Chem.* **79**, 1870–1874 (2001).

13. Freitag, R., Baltes, T. & Eggert, M. A comparison of thermoreactive water-soluble poly-*N,N*-diethylacrylamide prepared by anionic and by group transfer polymerization. *J. Polym. Sci., Part A: Polym. Chem.* **32**, 3019–3030 (1994).

14. Kobayashi, M., Okuyama, S., Ishizone, T. & Nakahama, S. Stereospecific anionic polymerization of *N,N*-diethylacrylamides. *Macromolecules* **32**, 6466–6477 (1999).

15. Kobayashi, M., Ishizone, T. & Nakahama, S. Synthesis of highly isotactic poly(*N,N*-diethylacrylamide) by anionic polymerization with Grignard reagents and diethylzinc. *J. Polym. Sci., Part A: Polym. Chem.* **38**, 4677–4685 (2000).

16. Katsumoto, Y., Etoh, Y. & Shimoda, N. Phase diagrams of stereocontrolled poly(*N,N*-diethylacrylamide) in water. *Macromolecules* **43**, 3120–3121 (2010).

17. Itakura, M., Inomata, K. & Nose, T. Aggregation behavior of poly(*N,N*-diethylacrylamide) in aqueous solution. *Polymer* **41**, 8681–8687 (2000).

18. Maeda, Y., Nakamura, T. & Ikeda, I. Change in solvation of poly(*N,N*-diethylacrylamide) during phase transition in aqueous solutions as observed by IR spectroscopy. *Macromolecules* **35**, 10172–10177 (2002).

19. Berry, G. C. Thermodynamic and conformational properties of polystyrene. I.

Light-scattering studies on dilute solutions of linear polystyrenes. *J. Chem. Phys.* **44**, 4550–4564 (1966).

20. Johnson, B. L. & Smith, J. in *Light Scattering from Polymer Solutions* (ed. Huglin, M. B.) Ch 2 (Academic Press, London, 1972).

21. Osa, M., Shiraki, H., Morinaga, U. & Yoshizaki, T. Effects of surfactants on cloud points in aqueous poly(*N*-isopropylacrylamide) solutions. *Polym. J*. **45**, 681–684 (2013).

22. Yamakawa, H. *Modern Theory of Polymer Solutions* (Harper & Row, New York, 1971).

23. Yamakawa, H. *Helical Wormlike Chains in Polymer Solutions* (Springer, Berlin, 1997).

24. Nakamura, Y. Dilute solution properties of star and comb polymers. *Kobunshi Ronbunshu* **57**, 530–541 (2000) and papers cited therein.

25. for example, Abe, F., Einaga, Y. & Yamakawa, H. Excluded-volume effects on the intrinsic viscosity of oligomers and polymers of styrene and isobutylene. *Macromolecules* **26**, 1891–1897 (1993).

Figure Captions

Figure 1. ^{13}C NMR spectra of the carbonyl carbon in the side group for the samples PDEA-T7, PDEA-T139, PDEA-B28, and PDEA-B122. The dashed, dot-dashed, and dotted curves represent the Lorentzian components for the *mm*, *mr*, and *rr* triads for each sample, respectively.

Figure 2. Double-logarithmic plots of $\langle S^2 \rangle$ (in nm^2) against M_w for PDEA in methanol at 25.0 °C: (○) PDEA-T samples; (△) PDEA-B samples. The solid straight line has a slope of 1.2.

Figure 3. Double-logarithmic plots of A_2 (in cm^3 mol/g^2) against M_w for PDEA in methanol at 25.0 °C: (○) PDEA-T samples; (△) PDEA-B samples. The solid straight line has a slope of −0.2.

Figure 4. Double-logarithmic plots of $[\eta]$ (in dL/g) against M_w for PDEA in methanol at 25.0 °C: (○) PDEA-T samples; (△) PDEA-B samples. The solid straight line has a slope of 0.7.

Figure 5. Temperature dependence of the transmittance of light passing through aqueous solutions of the samples PDEA-T7, PDEA-T11, PDEA-T27, PDEA-T40, PDEA-T80, and PDEA-T139 at w = 2.72, 3.01, 2.89, 3.02, 3.03, and 3.03 %, respectively. The horizontal line indicates the threshold value (90%) and the unfilled circle on each curve indicates the cloud point.

Figure 6. Temperature dependence of the transmittance of light passing through aqueous solutions of the samples PDEA-B18, PDEA-B28, PDEA-B85, and PDEA-B122, at w = 3.14, 3.00, 3.02, and 2.99 %, respectively. The horizontal line and the unfilled circles have the same meaning as those in Figure 5.

Figure 7. Cloud-point curves in aqueous solutions of the PDEA-T samples: (○) PDEA-T7, (△) PDEA-T11, (▽) PDEA-T27, (□) PDEA-T40, (◊) PDEA-T80, and (⊕) PDEA-T139. The solid curves smoothly connect the respective data points.

Figure 8. A photograph of the aqueous solution of the sample PDEA-T11 at *ca*. 10% and at *ca*. 34 °C, which exhibits the phase separation into two transparent liquid phases.

Figure 9. Cloud-point curves in aqueous solutions of the PDEA-B samples: (●) PDEA-B18, (▲) PDEA-B28, (▼) PDEA-B85, and (■) PDEA-B122. The solid curves smoothly connect the respective data points.

Figure 10. Plots of the critical point temperature against $M_w^{-1/2}$ for the aqueous PDEA solutions: (○) PDEA-T samples; (△) PDEA-B samples. The solid curve smoothly connects the data points for each kind of PDEA.

Table 1. Values of M_w/M_n and f_r and results of LS and viscosity measurements for two kinds of poly(*N*,*N*-diethylacrylamide) samples in methanol at 25.0 °C

sample	M_w/M_n	f_r	M_w	$10^4 A_2$ (cm^3 mol/g^2)	$10^{-2}\langle S^2\rangle$ (nm^2)	$[\eta]$ (dL/g)	k'
PDEA-T samples synthesized in *tert*-butanol							
PDEA-T4	1.20	–	3.85×10^4	5.47	–	–	–
PDEA-T7	1.20	0.60_5	6.95×10^4	4.56	–	–	–
PDEA-T11	1.14	–	1.14×10^5	4.04	–	–	–
PDEA-T16	1.10	–	1.57×10^5	3.61	–	0.440	0.40
PDEA-T20	1.09	–	2.06×10^5	3.42	–	–	–
PDEA-T27	1.12	–	2.69×10^5	3.21	2.99	0.658	0.35
PDEA-T40	1.10	–	3.98×10^5	2.83	4.80	0.839	0.32
PDEA-T55	1.16	–	5.52×10^5	2.72	7.73	–	–
PDEA-T59	1.10	–	5.87×10^5	2.58	9.06	–	–
PDEA-T67	1.22	–	6.70×10^5	2.49	10.8	–	–
PDEA-T80	1.30	–	7.99×10^5	2.33	12.3	1.32	0.36
PDEA-T139	1.12	0.61_9	1.39×10^6	2.14	24.0	2.18	0.32
PDEA-B samples synthesized in benzene							
PDEA-B18	1.23	–	1.77×10^5	3.37	–	0.473	0.32
PDEA-B28	1.16	0.51_7	2.81×10^5	2.94	4.12	0.729	0.40
PDEA-B39	1.21	–	3.86×10^5	2.85	6.35	–	–
PDEA-B51	1.12	–	5.08×10^5	2.71	9.30	1.12	0.36
PDEA-B63	1.15	–	6.27×10^5	2.43	11.3	–	–
PDEA-B85	1.24	–	8.54×10^5	2.20	16.2	–	–
PDEA-B115	1.22	–	1.15×10^6	2.11	22.8	1.64	0.38
PDEA-B122	1.23	0.51_9	1.22×10^6	2.04	24.9	–	–
PDEA-B158	1.26	–	1.58×10^6	1.82	38.4	2.33	0.41

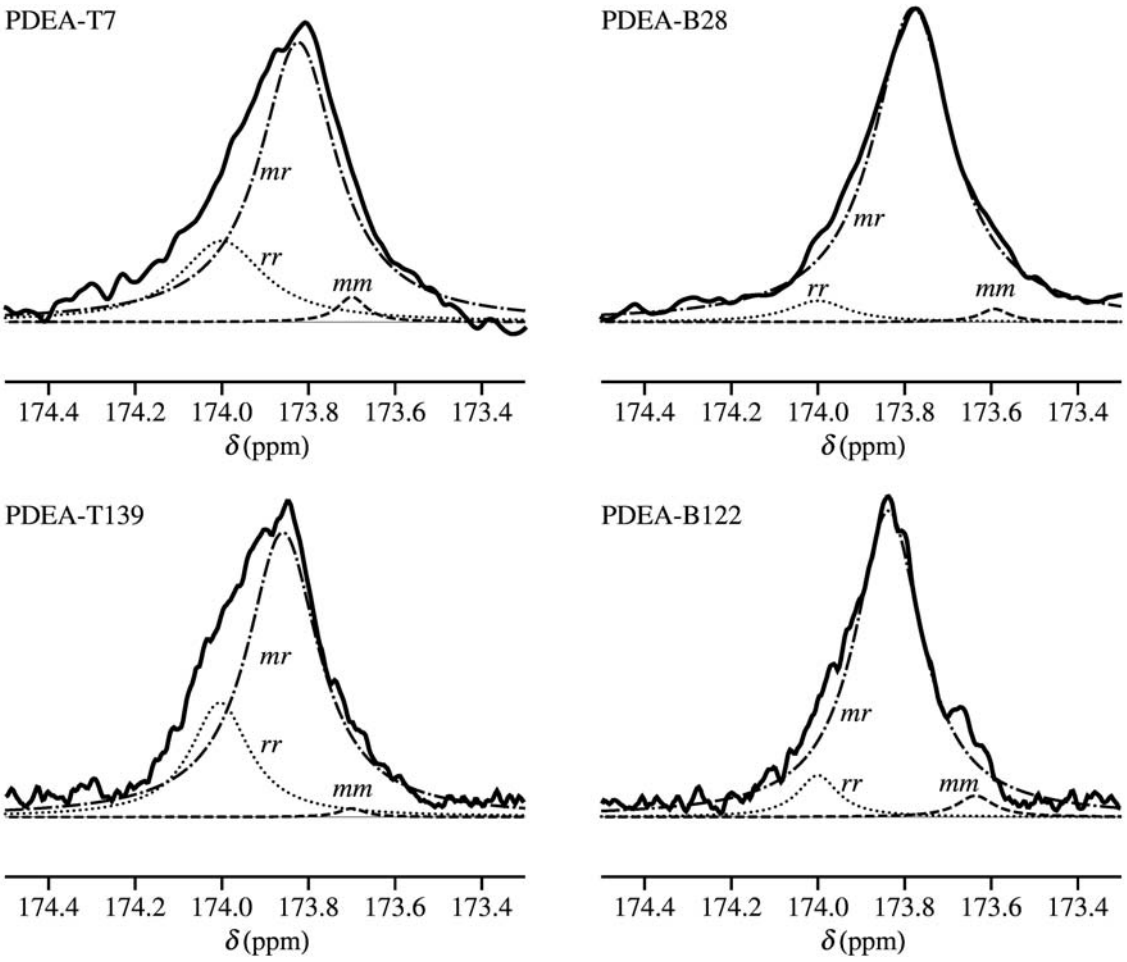

R. Watanabe *et al.*, Figure 1

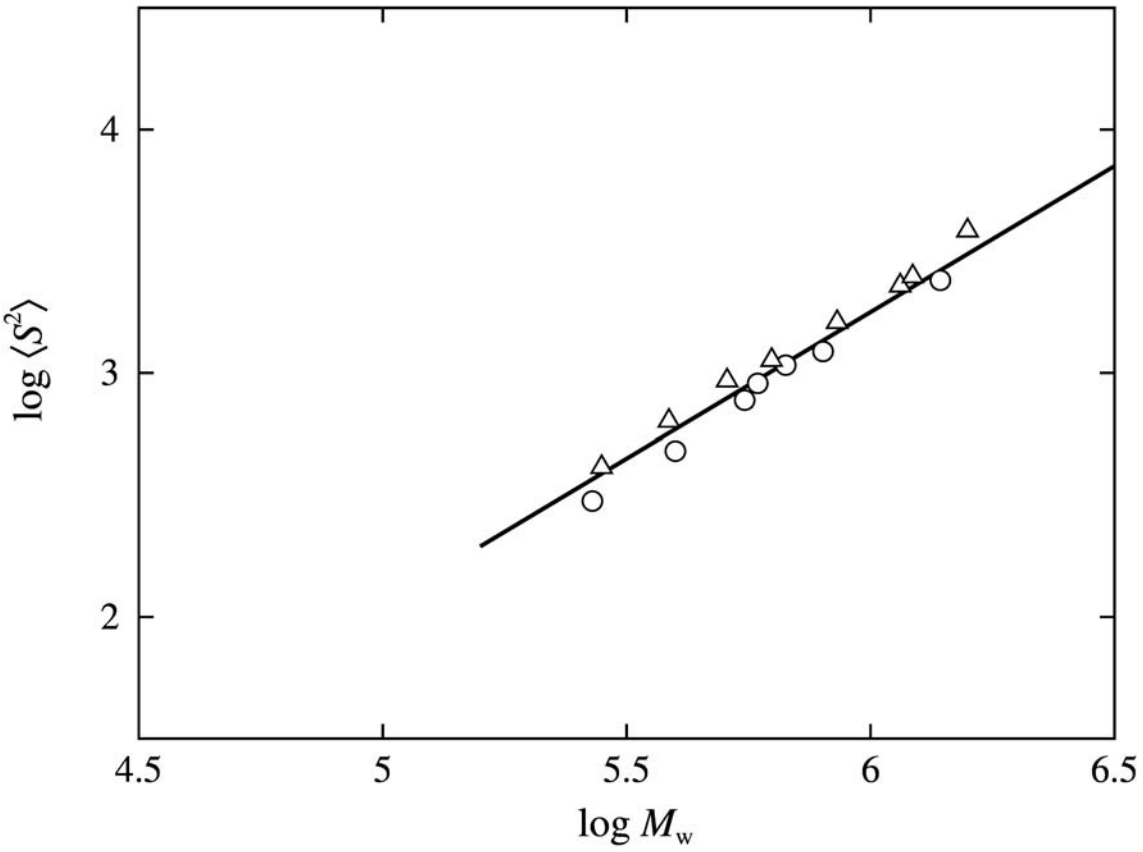

R. Watanabe *et al.*, Figure 2

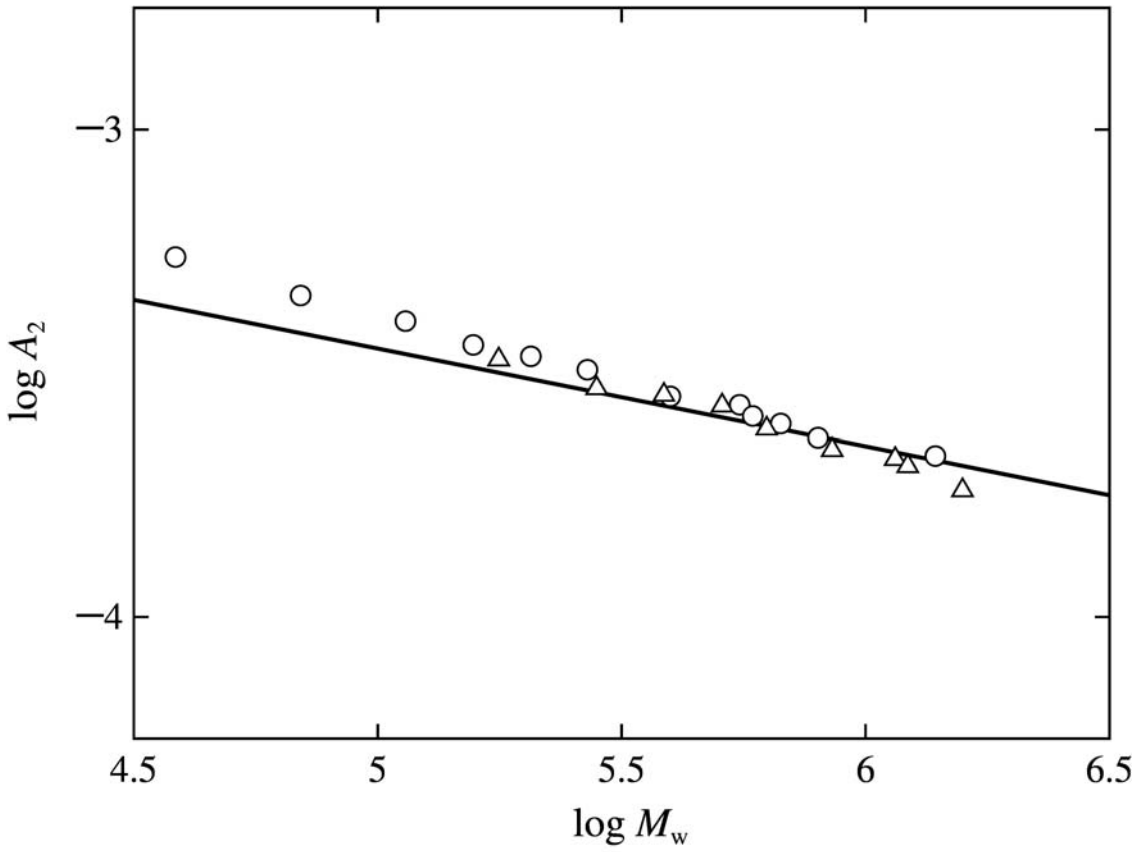

R. Watanabe *et al.*, Figure 3

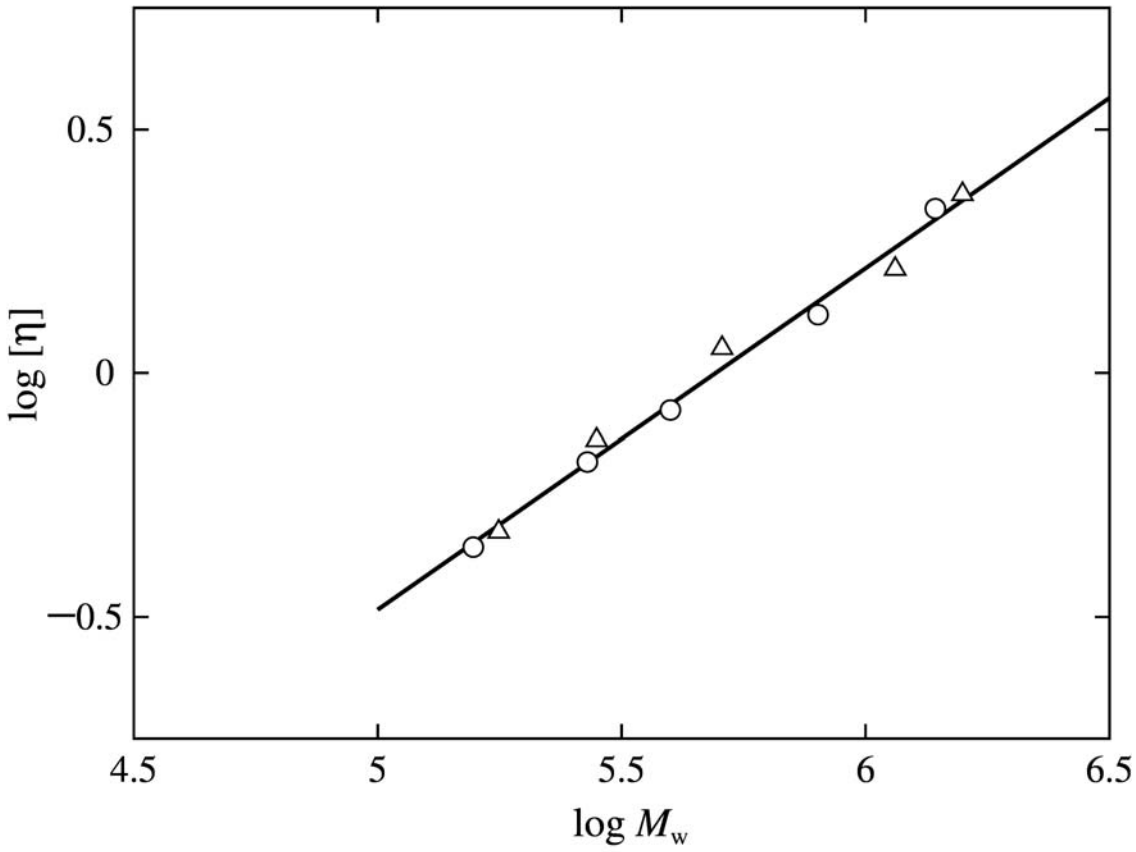

R. Watanabe *et al.*, Figure 4

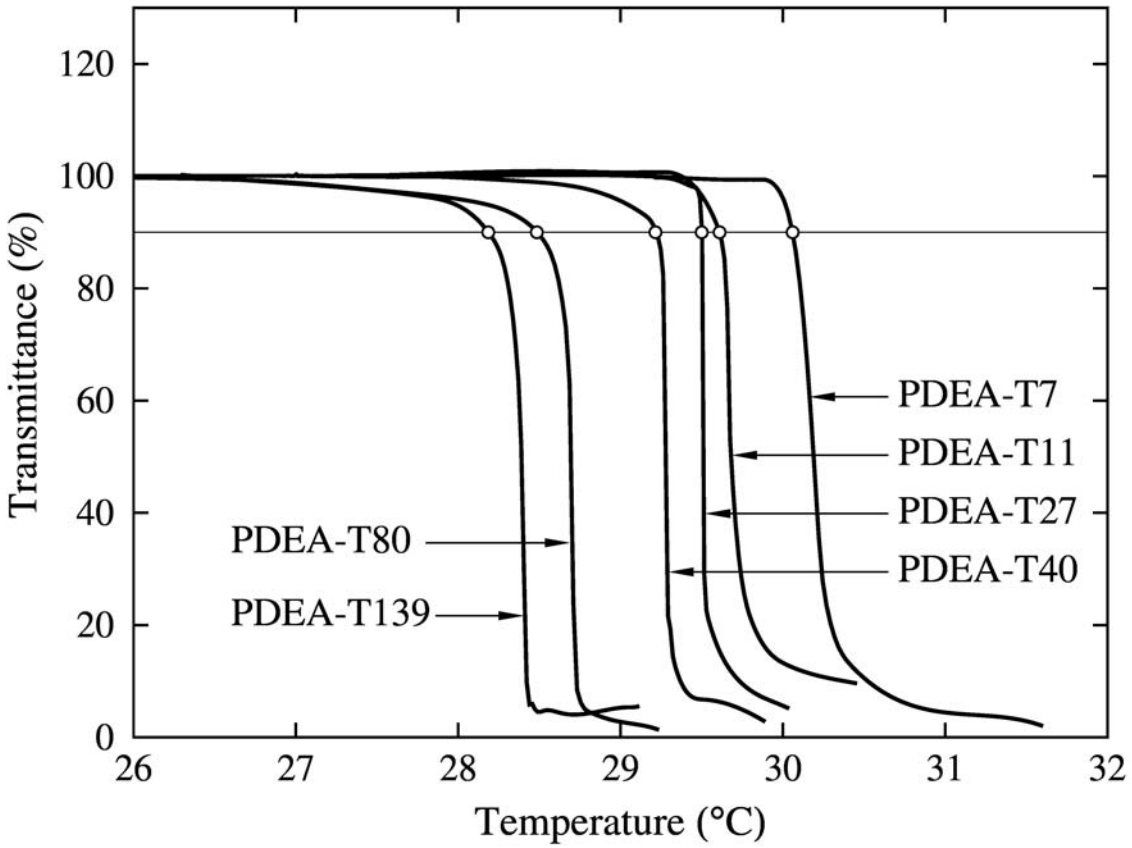

R. Watanabe *et al.*, Figure 5

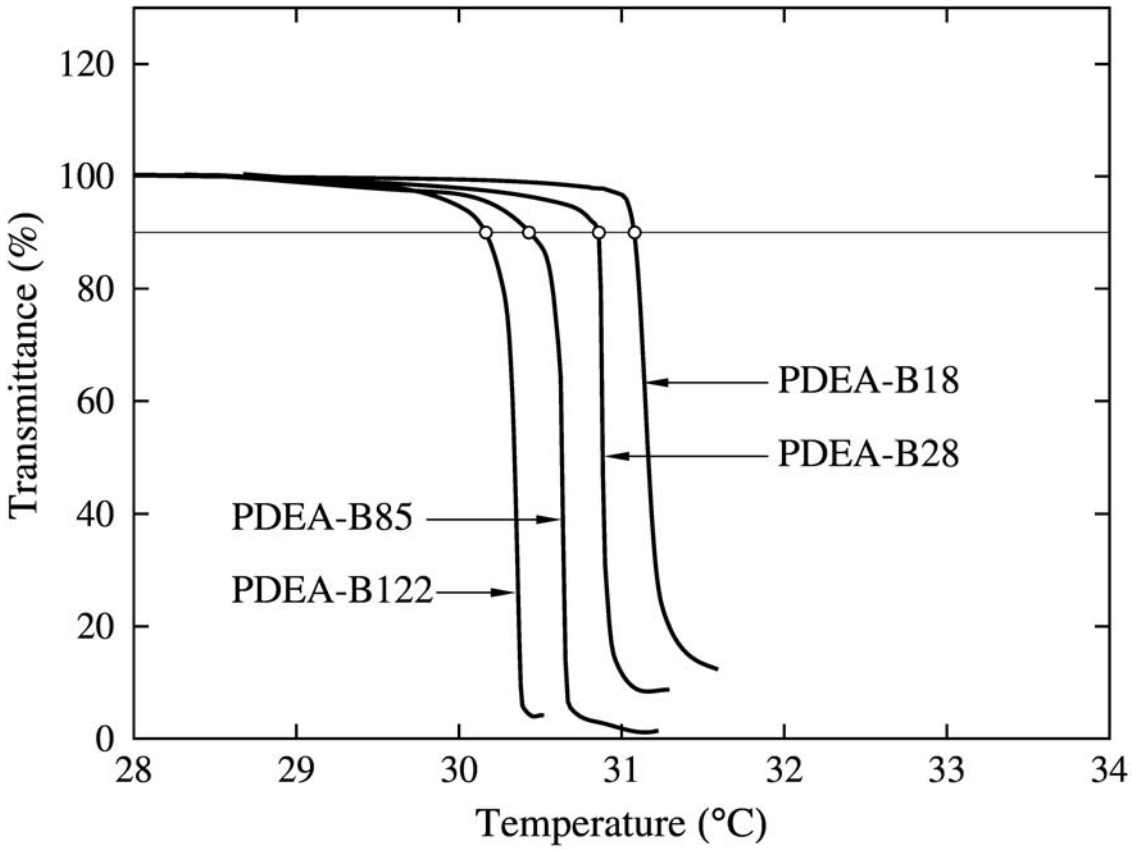

R. Watanabe *et al.*, Figure 6

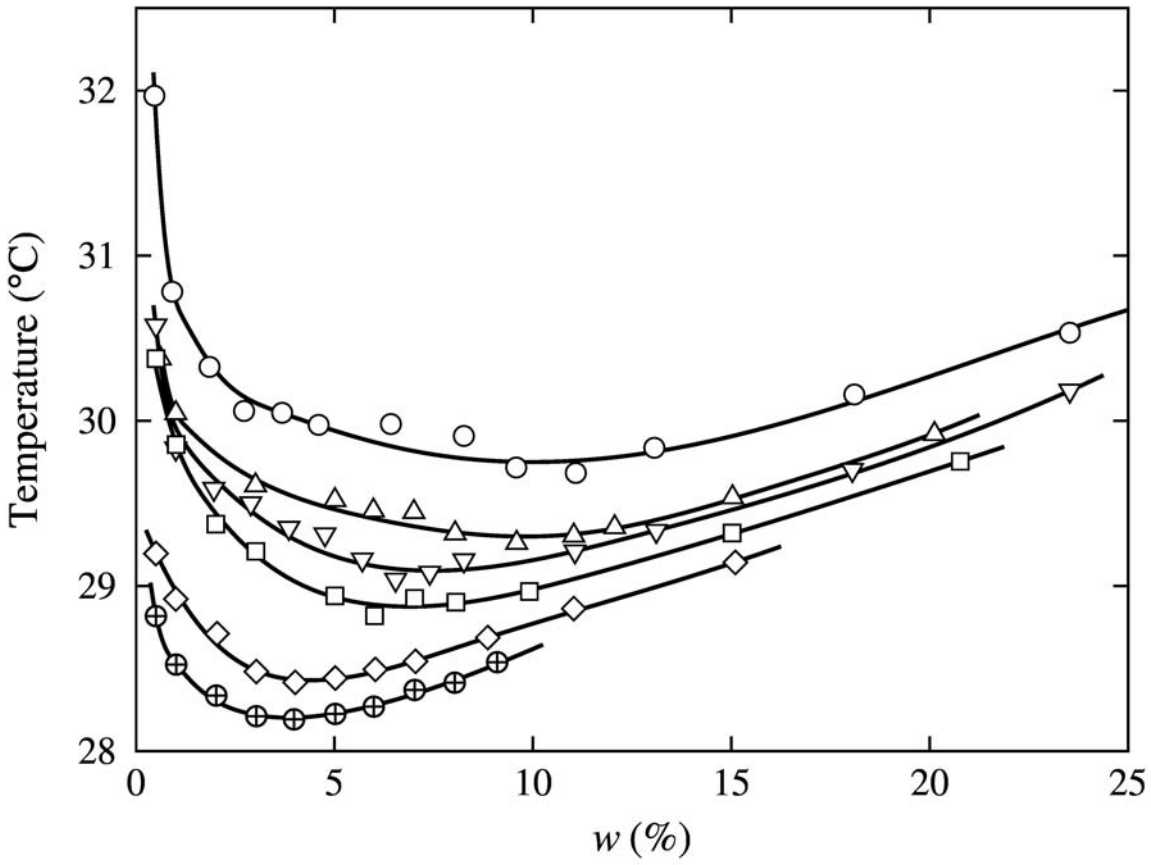

R. Watanabe *et al.*, Figure 7

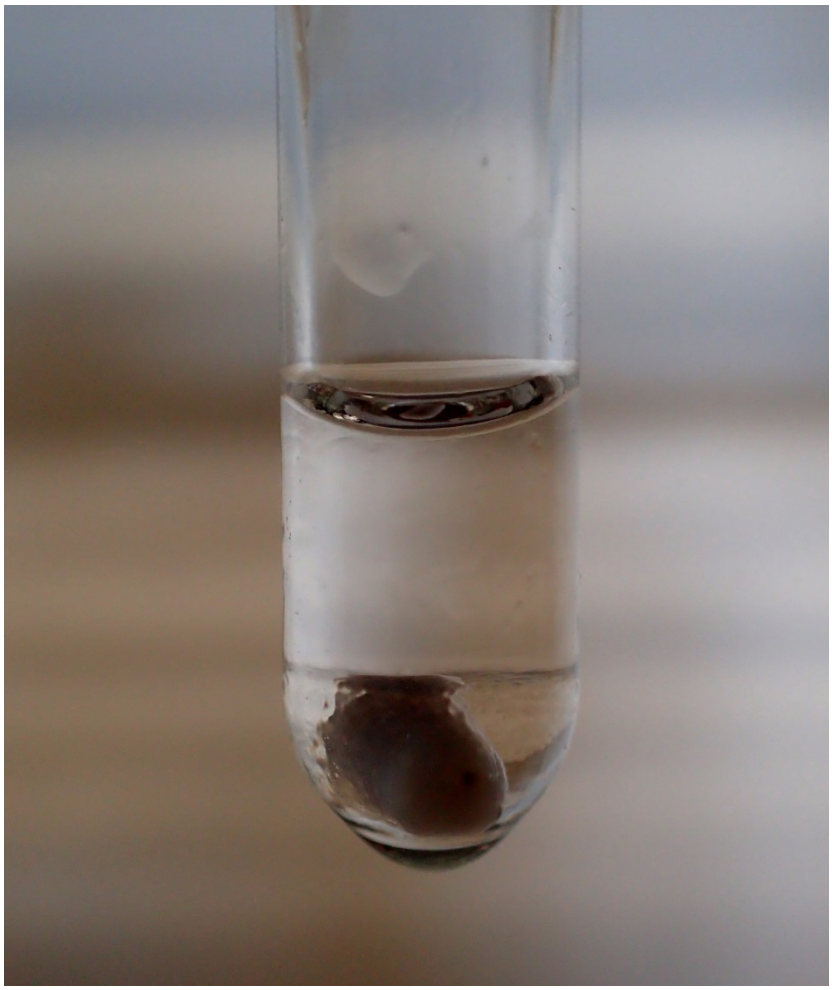

R. Watanabe *et al.*, Figure 8

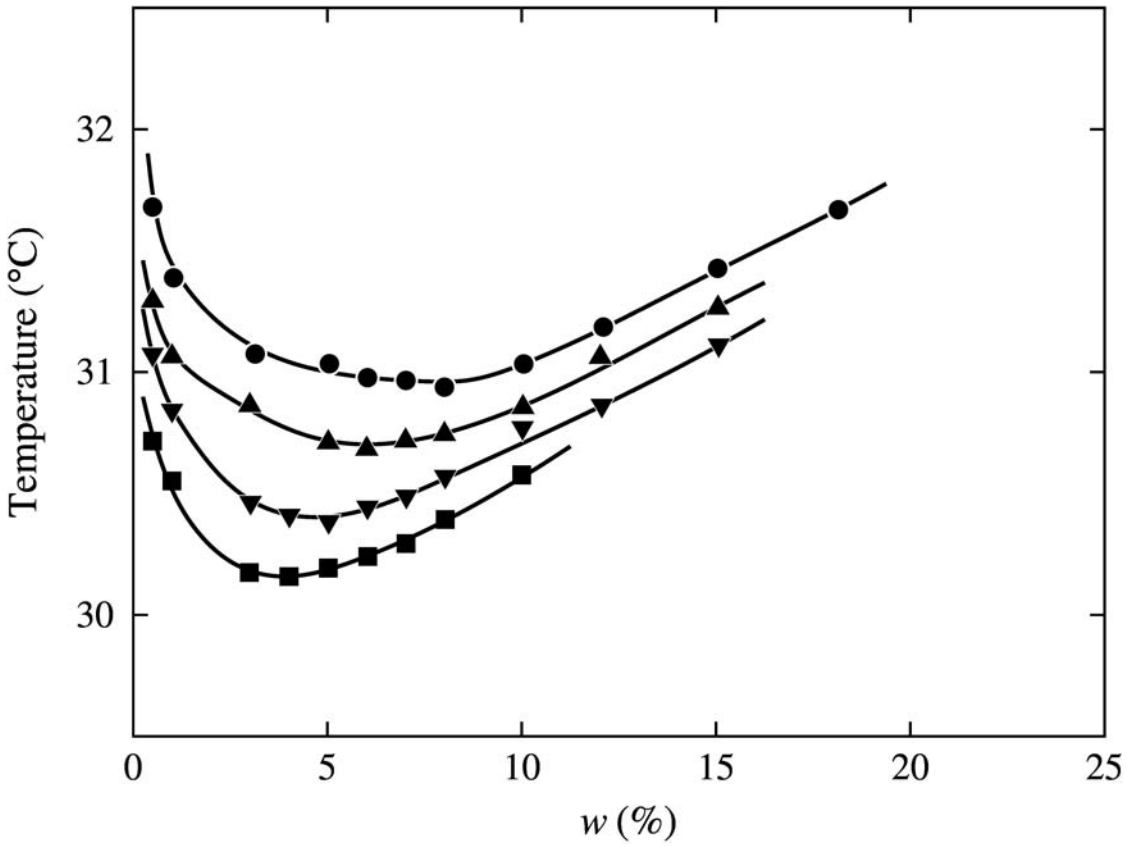

R. Watanabe *et al.*, Figure 9

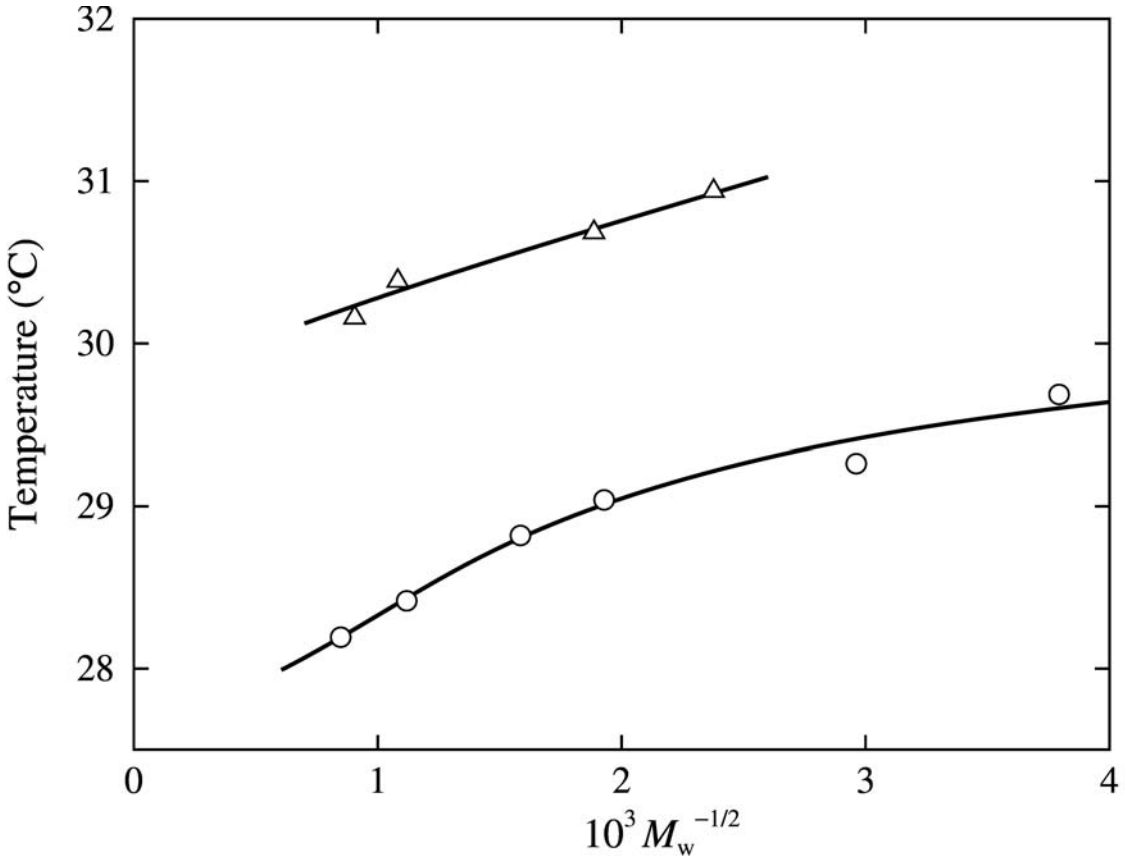

R. Watanabe *et al.*, Figure 10